Available online at www.sciencedirect.com

SciVerse ScienceDirect

Nuclear Physics A 904–905 (2013) 27c–34c

NUCLEAR PHYSICS A

www.elsevier.com/locate/nuclphysa

Overview of Recent ALICE Results

Karel Šafařík (for the ALICE Collaboration)[1]

CERN, Geneva

Abstract

An overview of the ALICE results obtained in Pb–Pb collisions at the LHC is presented. It covers identified-particle yields and spectra, azimuthal anisotropy and fluctuations, correlations and jets, heavy-flavour and charmonia production, and direct-photon production. This contribution is concluded with an outlook of the coming data-taking runs, and of the long-term plans for the upgrade of the ALICE detector.

1. Introduction

The ALICE collaboration was originated some twenty years ago, and since then its members have been developing, building and operating the largest dedicated heavy-ion detector. An ample effort went also into software development and performance studies. In November 2009 the ALICE detector recorded the first LHC collisions with proton beams, and in the falls of 2010 and 2011, during the first two heavy-ion runs, the ALICE experiment utilized respectively about $10\,\mu b^{-1}$ and $100\,\mu b^{-1}$ of integrated luminosity with Pb–Pb collisions at the centre-of-mass energy 2.76 TeV per nucleon pair. The LHC operated above expectations: during the second heavy-ion run the instant luminosity exceeded 10^{26} cm^{-2}s^{-1}, which is higher than the design value for that energy.

The ALICE detector is schematically shown in Fig. 1; it is composed of the following main parts: central barrel, muon arm, and forward detectors. The central barrel, which detects hadrons, electrons, and photons produced within about ±45° with respect to a plane perpendicular to the beam axis (corresponding to pseudorapidities $|\eta| < 0.9$), is placed inside a large solenoidal magnet with a magnetic field of 0.5 T. It comprises an Inner Tracking System (ITS) of high-resolution silicon detectors, a cylindrical Time-Projection Chamber (TPC), and particle identification arrays of Transition-Radiation Detectors (TRD) and of Time-Of-Flight (TOF) counters. Additional central subsystems, not-covering full azimuth, are a ring-imaging Čerenkov detector for High-Momentum Particle IDentification (HMPID), and two electromagnetic calorimeters: a high-resolution PHOton Spectrometer (PHOS) and a larger-acceptance ElectroMagnetic Calorimeter (EMCal). The muon arm detects muons emitted within 2°–9° from the beam axis (corresponding to $2.5 < \eta < 4$) and consists of a complex arrangement of absorbers, a dipole magnet with 3 Tm field integral, five pairs of tracking chambers, and two trigger stations. Several smaller detectors (VZERO, TZERO, FMD, ZDC, and PMD) for triggering, multiplicity measurements and centrality determination are installed in the forward region. The detailed layouts of the ALICE detector and of its subsystems are described in [1].

[1] A list of members of the ALICE Collaboration and acknowledgements can be found at the end of this issue.

0375-9474/

http://dx.doi.org/10.1016/j.nuclphysa.2013.01.041

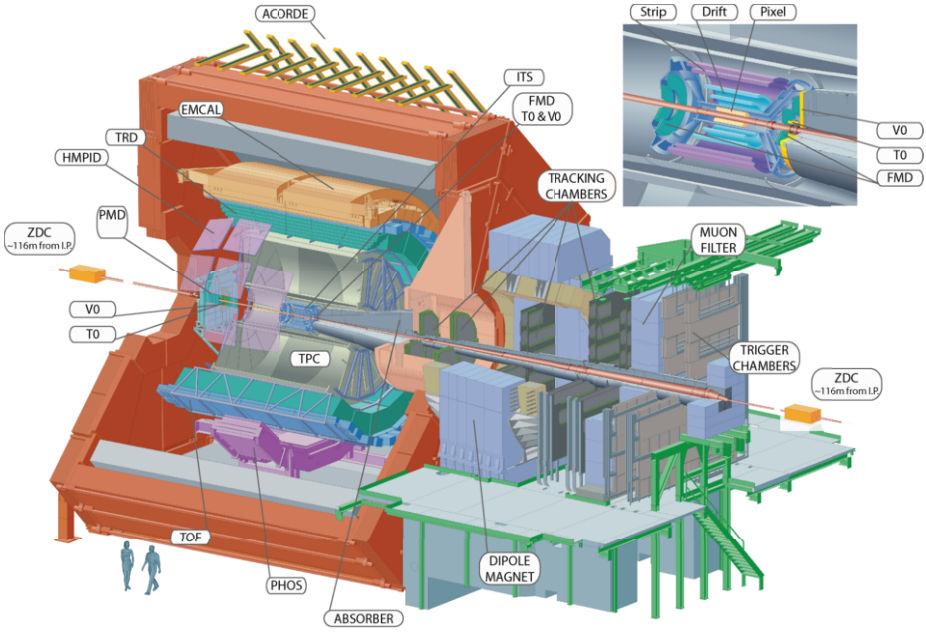

Figure 1: Schematic layout of the ALICE detector, indicating the main subsystems.

Nuclear collisions at the LHC produce events of enormous complexity with thousands of tracks, thus a robust and redundant tracking was from the beginning the design priority. To be able to study weak decays of heavy-flavour particles close to the interaction point, excellent vertexing capability was another key requirement. These were achieved by minimizing the amount of material in the sensitive tracking volume (about 10 % of radiation length between vertex and outer radius of the TPC), to reduce multiple scattering, and by installing the first tracking layer as close as possible to the interaction point (about 3.8 cm), to improve the pointing resolution. Another central features of the ALICE detector are its Particle IDentification (PID) systems capable to separate charged hadron species and electrons in a wide momentum range using practically all known PID techniques.

2. Recent Results

The ALICE results from the first two Pb–Pb LHC runs were summarized at this conference in six plenary talks [2, 3, 4, 5, 6, 7], and details were given in 30 parallel contributions and about 45 posters. Below, an overview of the highlights is given.

2.1. Particle Yields and Spectra

Transverse momentum (p_{T}) spectra of identified particles and their centrality dependence were measured by various techniques, such as specific ionization losses ($\mathrm{d}E/\mathrm{d}x$ with ITS and TPC), TOF, Čerenkov radiation, and topological decay reconstruction of strange particles. In order to obtain particle yields per rapidity unit the p_{T}-spectra are extrapolated and integrated

down to zero p_{T} using a blast-wave fit [8] or a Tsallis–Lévy parametrization [9]. The results for different particle species are shown in Fig. 2(left) compared to a thermal model prediction [10] with chemical freeze-out temperature $T_{\mathrm{ch}} = 164$ MeV and baryochemical potential $\mu_{\mathrm{b}} = 1$ MeV. The measured yields of protons and Λ's are significantly lower than those predicted by model calculations. When trying to adjust T_{ch} at the same μ_{b} to describe the data, the much lower temperature $T_{\mathrm{ch}} = 152$ MeV is obtained, and the fit does not reproduce the data well ($\chi^2 = 39.6$ per 9 d.o.f.) [11]. Fig. 2(right) shows the comparison of the particle yields normalized to that of pions with the measurement at lower energy at RHIC. At the LHC, both p/π and Λ/π ratios are below those measured at RHIC. A possible explanation of these deviations from the thermal-model predictions may be re-interactions in the hadronic phase; large cross sections for antibaryon–baryon annihilation can be at the origin of the lower yields of some baryons [12, 13]. The femtoscopic measurements of p–$\overline{\mathrm{p}}$ and Λ–$\overline{\Lambda}$ correlations, presented in [4, 14], are also relevant for this issue.

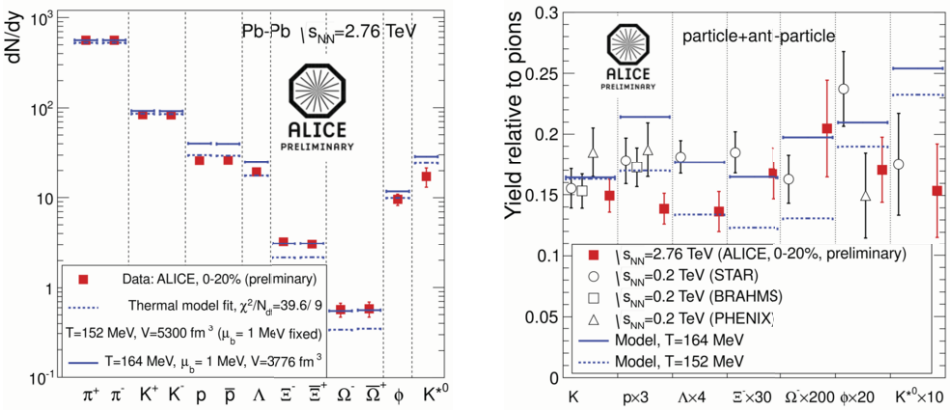

Figure 2: Yields per rapidity unit for different particle species measured in 20 % of most central Pb–Pb collisions at 2.76 TeV, compared to thermal model calculations (left). Relative yields, normalized to that of pions, compared to the values measured at RHIC in central Au–Au collision at 0.2 TeV by different experiments (right).

Identified charged-hadron p_{T}-spectra in the few-GeV/c region [8, 11] are harder than those measured at RHIC, indicating stronger radial flow. They are fairly well reproduced by calculations using a viscous hydrodynamical model coupled to hadron transport [15], or introducing non-equilibrium viscosity corrections at the transition from the hydrodynamical description to the hadronic one, effectively modifying T_{ch} [16]. At this conference, the p_{T}-spectra of charged pions, kaons and protons up to 20 GeV have been presented [2, 17]. The nuclear modification factor (R_{AA}) as a function of p_{T} (i.e. the p_{T} spectrum in Pb–Pb collisions normalized to the pp spectrum multiplied by number of binary nucleon–nucleon collisions corresponding to the Pb–Pb centrality selection) for identified hadrons exhibits, compared to $R_{\mathrm{AA}}(h^{\pm})$ for unidentified charged particles, the following behaviour:

- at p_{T} below $\simeq 7$ GeV/c: $R_{\mathrm{AA}}(\pi^{\pm}) < R_{\mathrm{AA}}(h^{\pm})$, $R_{\mathrm{AA}}(\mathrm{K}^{\pm}) \approx R_{\mathrm{AA}}(h^{\pm})$, and $R_{\mathrm{AA}}(\mathrm{p}) > R_{\mathrm{AA}}(h^{\pm})$;
- at higher p_{T} R_{AA} is compatible for all particles: $R_{\mathrm{AA}}(\pi^{\pm}) \approx R_{\mathrm{AA}}(\mathrm{K}^{\pm}) \approx R_{\mathrm{AA}}(\mathrm{p}) \approx R_{\mathrm{AA}}(h^{\pm})$.

This means that at high p_{T} (above $\simeq$ 10 GeV/c), where the particle production is suppressed in central Pb–Pb collisions by a large factor (more than 5 for 5 % most central collisions), the

particle composition does not change significantly with respect to pp collisions. However, in the p_{T} range of a few GeV/c, there is a clear hierarchy of suppression: the higher the particle mass – the less the suppression. Strong radial flow will qualitatively produce such behaviour. Another way to express the difference between pions and protons, is to plot the p/π ratio as a function of p_{T}. Compared to pp collisions, in 5 % of most central Pb–Pb collisions the p/π ratio is larger by a factor of 3 at a p_{T} of 3 GeV/c (the so called baryon anomaly), at higher p_{T}, the ratios get closer, and above 10 GeV/c the Pb–Pb ratio becomes compatible with the "normal" pp value. A similar observation was already reported by ALICE for the $\Lambda/\mathrm{K}^0_{\mathrm{s}}$ ratio. This effect persists to relatively large p_{T} values, and other explanations were proposed, such as particle production via quark recombination [18].

2.2. Flow and Fluctuations

Already the first measurements of the elliptic flow [19] confirmed that the dense hadronic matter created in nuclear collisions at the LHC is still a strongly-interacting, almost perfect liquid as observed at RHIC, well described by hydrodynamical calculations with very low viscosity. Since then many new results have been reported in this field [3]: flow for identified particles, higher azimuthal harmonics, directed flow, high-p_{T} flow, rapidity dependence, and a new approach related to the study of fluctuations – "event shape engineering" [20].

The elliptic-flow coefficient v_2 for different particle species, normalized to the number of constituent quarks (n_{q}), is shown in Fig. 3 as a function of the transverse kinetic energy per constituent quark. This picture of n_{q} scaling is not as good as observed at RHIC, there is still an indication of a residual splitting in low-p_{T} region (below 3 GeV/c), and at higher p_{T} the differences in v_2/n_{q} are 10–20 %, especially for semi-peripheral collisions (40–50 % centrality class). However, qualitatively the mass dependence of v_2 up to 2–3 GeV/c is still described by hydrodynamical models with hadronic afterburners [21]. The results for multi-strange baryons (Ξ^- and Ω^-) were also reported [22].

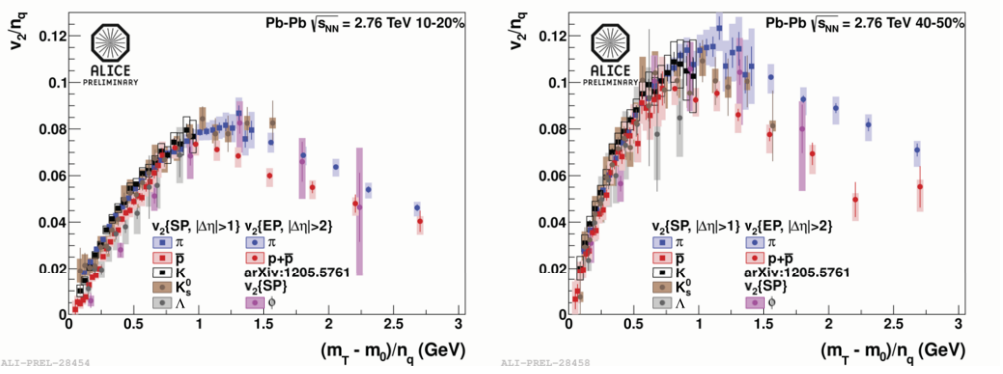

Figure 3: Elliptic-flow coefficient v_2 per constituent quark as a function of transverse kinetic energy ($m_{\mathrm{T}} - m_0$, where $m_{\mathrm{T}} = \sqrt{m_0^2 + p_{\mathrm{T}}^2}$) per constituent quark for different particle species. The left side is for centrality 10–20 %, the right side for centrality 40–50 %.

When comparing to the RHIC experiments, ALICE has extended the measurements of the azimuthal anisotropy both in rapidity and p_{T}. Data on v_2 and v_3 were presented up to $\eta = 5$ [23]; there is a plateau observed for $|\eta| < 2$. When comparing to the PHOBOS v_2 measurement [24],

applying a shift by beam rapidity, the longitudinal scaling observed at RHIC is confirmed. The harmonic coefficients v_2, v_3, and v_4 were measured up to a p_T of 20 GeV/c. Non-flow contributions are suppressed by using a pseudorapidity gap or higher-cumulant methods. The elliptic-flow coefficient v_2 remains non-zero up to the highest p_T, where its value is well reproduced by a model that includes an azimuthal dependence of jet quenching [25]. The higher harmonics are compatible with zero at p_T above 10 GeV/c, possibly indicating the disappearance of fluctuations at high p_T [3].

At a fixed centrality the ensemble of nuclear events exhibits a large spread in flow, one can select event samples with predefined flow fluctuations and study their differences in other variables. The first results using this event-shape-engineering method indicate very similar initial shape fluctuations up to p_T 6–8 GeV/c [3, 11, 26].

2.3. Correlations and Jets

The particle composition in jet-like structures, selected with particle correlations in $\Delta\varphi$ (difference in azimuthal angle) and $\Delta\eta$ (difference in pseudorapidity) to a trigger particle with p_T in the range 5–10 GeV/c, is studied by measuring p/π ratio in [4, 27]:

- "bulk" – a region far from the trigger particle;
- "peak" – particles close in $\Delta\varphi$–$\Delta\eta$ to the trigger particle;
- "jet" ("peak" − "bulk") obtained by correcting the "peak" p/π ratio for the contribution of the underlying event (using the "bulk" value) according to the relative population in the correlation peak above the underlying background.

The p/π ratio in the bulk region, obtained in this analysis in the p_T range 1.5–4.5 GeV/c, coincides with the values for non-triggered Pb–Pb events of the same centrality, i.e. the ratio increases by up to 3 times compared to pp interactions (cf. Section 2.1). However, the jet p/π ratio is as expected for pp collisions from PYTHIA calculations, indicating that the jet particle composition may not be modified in the medium. To understand the medium influence on jet fragmentation, further studies are needed, including a measurement of the particle composition on the away side of the correlation peak, to avoid a surface bias.

The evolution of the shape of the near-side correlation peak with the collision centrality is studied by measuring the width of the peak in the $\Delta\varphi$ and $\Delta\eta$ directions [4, 28]. The width in the longitudinal direction ($\Delta\eta$) shows a strong centrality dependence, increasing by a factor about 1.6 from peripheral to central Pb–Pb collisions; contrary to that, the width in the azimuthal direction ($\Delta\varphi$) has a much weaker, if any, centrality dependence. Such a behaviour is expected in a model taking into account the interaction of the fragmenting jet with the longitudinally flowing medium [29]. Interestingly, the AMPT model [30] calculations exhibit a very similar centrality dependence of the near-side peak.

The jet transverse-energy spectrum, reconstructed with charged particles having p_T down to 150 MeV/c and using the anti-k_T algorithm, is compared to that calculated for pp collisions with the PYTHIA model [5, 31]. The observed jet energy has to be corrected for the contamination due to the underlying event; fluctuations of this background are taken into account by deconvoluting the measured distributions for the jets and for the underlying event. The resulting nuclear modification factor indicates a very strong suppression of jet production, similar to that of inclusive charged particles. The transverse-energy dependence of the jet suppression in the measured range (30–110 GeV) is well described by the JEWEL model [32].

2.4. Heavy-Flavour and Quarkonia

The measurements of the D-meson nuclear modification factor have been extended up to p_{T} 36 GeV/c [6, 33]. The average R_{AA} for prompt D, D^{+}, and D^{*+} at p_{T} below 8 GeV/c is found to be slightly higher than the charged-particle R_{AA}; however, the effect is still within the systematic uncertainties. At higher p_{T}, the suppression for charm mesons is very similar to that observed for charged particles (mostly light hadrons). As the latter are supposed to be produced at LHC energies mostly in gluon fragmentation and the former mostly in quark fragmentation, there is no indication for a colour-charge dependence of the suppression factor. Different model calculations can describe the measured data [25, 34, 35, 36].

The suppression of heavy-flavour production is also studied exploiting their semi-leptonic decays, detecting electrons in the central barrel and muons in the forward muon arm [37, 38]. The lepton spectra, which at higher p_{T} are dominated by B particles, qualitatively confirm the observations obtained for exclusive D decays. The first result on $\mathrm{D}_{\mathrm{s}}^{+}$ measurement in heavy-ion collisions was presented [39]. The nuclear modification factor has very large uncertainties, the central values for p_{T} below 8 Gev/c being above those for other D mesons. This measurement will improve with future data takings.

The J/ψ suppression is measured both at mid- (dielectrons) and forward- (dimuons) rapidity [7, 40, 41]. For collisions with a number of participants above $\simeq$ 100 the suppression is practically constant, and for the most central collisions, the J/ψ is less suppressed than at RHIC. At low p_{T} (below 2 GeV/c) a smaller suppression is observed than for p_{T} in the region 5–8 GeV/c, especially for the most central collisions. Such a behaviour is expected in models with J/ψ (re)generation. Numerical calculations show that both regeneration [42] and statistical hadronization [43] models can reproduced the measured data. The estimate of the ψ(2S) yield in the forward region at p_{T} above 3 GeV/c does not confirm a possible enhancement of the ψ(2S)/(J/ψ) ratio in central Pb–Pb collisions with respect to pp data, as previously reported by the CMS collaboration [44].

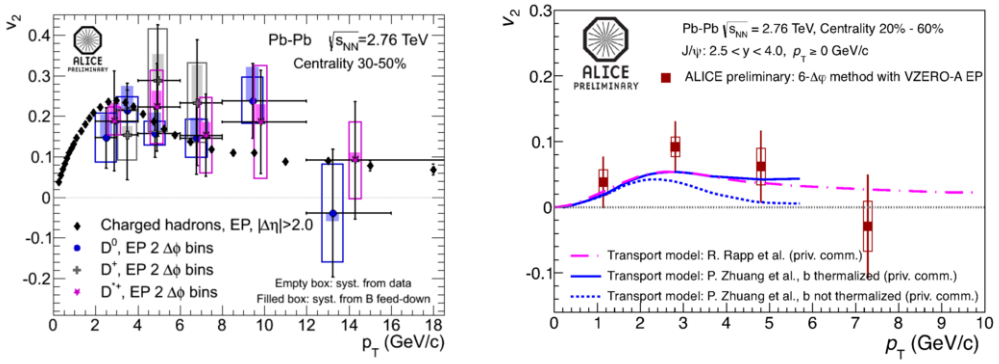

Figure 4: Elliptic-flow coefficient v_2 as a function of p_{T} for different D mesons together with the measurement for charged hadrons (left), and for J/ψ compared to model calculations (right).

The measurements of the elliptic-flow coefficient v_2 in the heavy-flavour sector were also reported. In Fig. 4(left) the D-meson v_2 is compared to the v_2 measured for charged particles [45]. There is an indication for non-zero v_2 for charm mesons, the value being comparable with that for light hadrons. There is also a hint of non-zero v_2 for J/ψ observed in forward region, see Fig. 4(right) [46]. Both these elliptic-flow measurements indicate possible thermalization of

charm quarks in the hot matter created at the LHC, and they will be improved with future heavy-ion data taking. A challenge for theory will be the simultaneous description of the R_{AA} and v_2 data.

2.5. Direct Photons

ALICE presented results on direct photon p_T-spectra using the measurement of γ conversions [47]. Figure 5(left) shows the double ratio: measured γ_{inc}/π^0 in 40 % of most central Pb–Pb collisions over γ_{decay}/π^0 from a cocktail calculation. The excess over unity is the direct-photon signal, which at p_T above 4 GeV/c is well reproduced by the NLO pQCD prediction for pp collisions, scaled by the number of binary collisions. However, at around 2 GeV/c there is about 20 % excess, attributed to thermal photons. The corresponding p_T-spectrum of direct photons is shown in Fig. 5(right) together with the scaled NLO prediction and the exponential fit in the p_T range 0.8–2.2 GeV/c. The inverse slope of this exponential is extracted as $T = (304 \pm 51)$ MeV, where the quoted error includes both the statistical and systematic uncertainties. The LHC value is about 40 % higher than that measured in a similar analysis at RHIC by PHENIX [48].

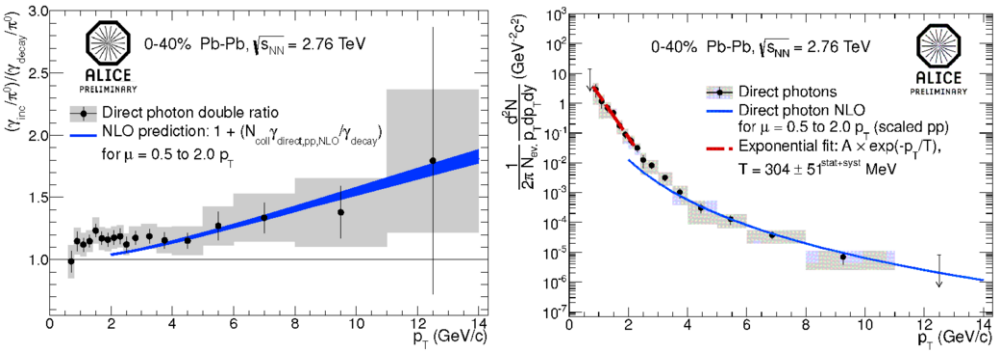

Figure 5: Double ratio of measured γ_{inc}/π^0 in 40 % most central Pb–Pb collisions over γ_{decay}/π^0 from a cocktail calculation (left). The line corresponds to the NLO pQCD calculation scaled by number of binary collisions. Direct-photon p_T-spectrum with NLO prediction and exponential fit in low-p_T region (right).

3. Summary and Outlook

After having confirmed the main discoveries made at SPS and RHIC, ALICE has entered an exciting phase of new measurements, allowing a much broader and deeper study of strongly interacting hadronic matter. At the same time, ALICE is already preparing, on the basis of what has been learnt so far, the next steps for a more detailed characterization of the extreme state of matter produced at the LHC.

The coming heavy-ion running period was recently re-scheduled for January 2013, and will be dedicated to p–Pb collisions. Then the LHC operation will be paused for an upgrade necessary to increase the collision energy. After the restart, the ALICE collaboration aims to complete its approved programme, collecting 1 nb^{-1} of heavy-ion collisions at the higher collision energy, 5.5 TeV per nucleon pair. The intention is to complete a significant part of this programme before the second long shutdown for the LHC luminosity increase, planned for 2018. ALICE detector upgrade [49, 50] allowing for high-luminosity heavy-ion running after this period is

currently under approval. An extended physics programme, justifying the LHC operation in heavy-ion mode until the mid-2020s, which would imply collecting over 10 nb^{-1} of data, has been prepared [51].

References

[1] K. Aamodt et al. (ALICE Collaboration), J. Instrum. 3, S08002 (2008).
[2] M. Ivanov (ALICE Collaboration), this proceedings.
[3] S.A. Voloshin (ALICE Collaboration), this proceedings.
[4] A.M. Adare (ALICE Collaboration), this proceedings.
[5] A. Morsch (ALICE Collaboration), this proceedings.
[6] Z. Conesa del Valle (ALICE Collaboration), this proceedings.
[7] E. Scomparin (ALICE Collaboration), this proceedings.
[8] B. Abelev at al. (ALICE Collaboration), arXiv:1208.1974[hep-ex], to be published in Phys. Rev. Lett.
[9] S. Singha (ALICE Collaboration), this proceedings.
[10] A. Andronic, P. Braun-Munzinger, and J. Stachel, Phys. Lett. B673, 142 (2009).
[11] L. Milano (ALICE Collaboration), this proceedings.
[12] F. Becattini et al., arXiv:1203.5302[nucl-th] (2012).
[13] J. Steinheimer, J. Aichelin, and M. Bleicher, arXiv:1203.5302[nucl-th] (2012).
[14] M. Szymanski (ALICE Collaboration), this proceedings.
[15] Yu. Karpenko, Yu. Sinyukov, and K. Werner, arXiv:1204.5351[nucl-th] (2012).
[16] P. Bozek, Phys. Rev. C85, 034901 (2012).
[17] A. Ortiz Velasquez (ALICE Collaboration), this proceedings.
[18] R.J. Fries et al., Phys. Rev. Lett. 90, 202303 (2003), Phys. Rev. C68, 044902 (2003).
[19] K. Aamodt et al. (ALICE Collaboration), Phys. Rev. Lett. 105, 252302 (2010).
[20] J. Schukraft, A. Timmins and S.A. Voloshin, arXiv:1208.4563[nucl-ex] (2012).
[21] U.W. Heinz, C. Shen and H. Song, AIP Conf. Proc. 1441, 766 (2012).
[22] F. Noferini (ALICE Collaboration), this proceedings.
[23] A. Hansen (ALICE Collaboration), this proceedings.
[24] B.B. Back et al. (PHOBOS Collaboration), Phys. Rev. Lett. 94, 122303 (2005).
[25] W.A. Horowitz and M. Gyulassy, J. Phys. G 38, 124114 (2011).
[26] A. Dobrin (ALICE Collaboration), this proceedings.
[27] J.G. Ulery (ALICE Collaboration), this proceedings.
[28] F. Krizek (ALICE Collaboration), this proceedings.
[29] N. Armesto, C. Salgado, and U.A. Wiedemann, Phys. Rev. Lett. 93, 242301 (2004).
[30] Z.-W. Lin et al., Phys. Rev. C72, 064901, (2005).
[31] R. Reed (ALICE Collaboration), this proceedings.
[32] K.C. Zapp, F. Krauss, and U.A. Wiedemann, arXiv:1111.6838[hep-ph] (2011).
[33] A. Grelli (ALICE Collaboration), this proceedings.
[34] R. Sharma et al., Phys. Rev. C80, 054902 (2009).
[35] N. Armesto et al., Phys. Rev. D71 054027 (2005).
[36] A. Beraudo, J.G. Milhano, and U.A. Wiedemann, J. Phys. G 38 124144 (2011).
[37] X. Zhang (ALICE Collaboration), this proceedings.
[38] S. Sakai (ALICE Collaboration), this proceedings.
[39] G.M. Innocenti (ALICE Collaboration), this proceedings.
[40] I. Arsene (ALICE Collaboration), this proceedings.
[41] R. Aranldi (ALICE Collaboration), this proceedings.
[42] X. Zhao and R. Rapp, Nucl. Phys. A859, 114 (2011).
[43] A. Andronic et al., J. Phys. G 38, 124081 (2011).
[44] T. Dahms (CMS collaboration), presentation at Hard Probes 2012, Cagliari, May 2012.
[45] D. Caffarri (ALICE Collaboration), this proceedings.
[46] H. Yang (ALICE Collaboration), this proceedings.
[47] M. Wilde (ALICE Collaboration), this proceedings.
[48] A.M. Adare et al. (PHENIX Collaboration), Phys. Rev. Lett. 104, 132301 (2010).
[49] Th. Peitzmann (ALICE Collaboration), this proceedings.
[50] R.C. Lemmon (ALICE Collaboration), this proceedings.
[51] ALICE Collaboration, CERN-LHCC-2012-012 (2012).